

# Effects of MgO doping in ZnO–0.5 mol% V<sub>2</sub>O<sub>5</sub> varistors

H.H. Hng<sup>\*</sup>, K.Y. Tse

*School of Materials Science & Engineering, Division of Materials Science, Nanyang Technological University, Nanyang Ave,  
Singapore 639798, Singapore*

Received 3 October 2006; received in revised form 16 January 2007; accepted 10 February 2007

Available online 6 March 2007

## Abstract

The effects of MgO (0–40 mol%) on the microstructure and the electrical properties have been studied in a binary ZnO–0.5 mol% V<sub>2</sub>O<sub>5</sub> system. The microstructure of the samples consists mainly of ZnO grains with MgO and  $\gamma$ -Zn<sub>3</sub>(VO<sub>4</sub>)<sub>2</sub> as the minority secondary phases. MgO is found to be effective as a grain growth inhibitor in controlling the ZnO grain growth, and a more uniform microstructure can be obtained. The non-linear coefficient  $\alpha$  value is found to increase with the amount of MgO, and a highest value of 8.7 is obtained for the sample doped with 10 mol% MgO. Further addition of  $\geq 20$  mol% MgO decreases the  $\alpha$  value.

© 2007 Elsevier Ltd and Techna Group S.r.l. All rights reserved.

**Keywords:** B. Microstructure-final; D. ZnO; D. MgO; E. Varistors; V<sub>2</sub>O<sub>5</sub>

## 1. Introduction

ZnO varistors derive their non-linear current–voltage behaviour from the addition of small amounts of other metal oxides, such as Bi<sub>2</sub>O<sub>3</sub>, Pr<sub>6</sub>O<sub>11</sub>, MnO<sub>2</sub> and Co<sub>3</sub>O<sub>4</sub> [1,2]. It is generally believed that effective varistor forming ingredients are heavy elements with large ionic radii, such as Bi and Pr, which segregate to grain boundaries and form intergranular phases [3,4]. However, studies have shown that relatively light element vanadium is also a potential varistor former, since ZnO–V<sub>2</sub>O<sub>5</sub> system exhibits varistor behaviour, similar to that of ZnO–Bi<sub>2</sub>O<sub>3</sub> system [5–8]. The ZnO–V<sub>2</sub>O<sub>5</sub> system is of interest because the ceramic can be sintered at a relatively low temperature of about 900 °C.

ZnO varistors exhibit non-linear current–voltage ( $I$ – $V$ ) characteristics and other electrical properties that are directly related to their microstructure, specifically the ZnO grain size that affects the varistor breakdown voltage per unit thickness [1–4]. To achieve a given breakdown voltage, one can change either the varistor thickness or the grain size by using grain growth inhibitors. Sb<sub>2</sub>O<sub>3</sub> is a commonly used grain growth inhibitor for Bi<sub>2</sub>O<sub>3</sub>-doped ZnO varistors [2]. However, it has been shown that the use of Sb<sub>2</sub>O<sub>3</sub> in V<sub>2</sub>O<sub>5</sub>-doped ZnO varistor

requires a high sintering temperature of 1200 °C in order for the pellet to be sintered [8]. MgO is another oxide which has been reported to control grain growth in Bi<sub>2</sub>O<sub>3</sub>-doped ZnO varistors [9]. Hence, in this work, the feasibility of using MgO to control grain growth in V<sub>2</sub>O<sub>5</sub>-doped ZnO varistors will be studied. In addition, its effects on the final microstructure and current–voltage behaviour of the varistor will also be investigated.

## 2. Experimental procedure

High purity oxide powder starting materials were used for the preparation of the ZnO varistor samples. MgO, in the range of 0–40 mol%, was mixed with a mixture of ZnO–0.5 mol% V<sub>2</sub>O<sub>5</sub> powder by ball milling with alumina balls and deionised water for 24 h. The mixtures were then dried, pressed into pellets, and sintered in an atmosphere of ambient air for 4 h at 1000 °C and cooled at 5 °C/min.

For electrical measurements, the as-sintered specimens were lapped on both surfaces to ensure flat and parallel surfaces. They were coated with conductive silver paint on both surfaces, then heat cured to provide ohmic contacts. The current–voltage ( $I$ – $V$ ) characteristics were determined at room temperature using a variable dc power supply (Kikusui Withstanding Voltage Tester, TOS 5051). X-ray diffraction analysis of the sintered samples was carried out using Cu K $\alpha$  radiation on a Shimadzu Lab X-ray diffractometer. Microstructures were

<sup>\*</sup> Corresponding author. Tel.: +65 67904140; fax: +65 67909081.

E-mail address: [ashhhng@ntu.edu.sg](mailto:ashhhng@ntu.edu.sg) (H.H. Hng).

examined by SEM (JEOL JSM 5310) equipped with energy dispersive X-ray analysis (EDX).

### 3. Results and discussion

#### 3.1. X-ray diffraction (XRD)

Typical XRD traces for undoped and doped MgO samples are shown in Fig. 1. In all the samples, ZnO was the main phase and only very small quantities of secondary phases were detected. In agreement with previous work on  $V_2O_5$ -doped ZnO ceramics [5–8], these secondary phases were found to be zinc vanadates. Brown and Hummel [10] identified three zinc orthovanadates,  $Zn_3(VO_4)_2$ , which they designated as  $\alpha$ ,  $\beta$  and  $\gamma$ . However, later studies [11,12] have queried the existence of polymorphism in  $Zn_3(VO_4)_2$ , and it was confirmed that neither  $\beta$ - nor  $\gamma$ - $Zn_3(VO_4)_2$  phases exist. In fact, it was deduced that the  $\beta$ -phase is actually  $Zn_4V_2O_9$  (JCPDS 77-1757) phase, and the  $\gamma$ -phase (JCPDS 19-1470) could be an oxide compound composed of zinc, vanadium and manganese or it can be a mixture of zinc vanadates.  $Zn_4V_2O_9$  was detected in the binary ZnO– $V_2O_5$  sample that is not doped with MgO, which agrees with our previous work [8]. However, for samples containing MgO, the  $\gamma$ - $Zn_3(VO_4)_2$  was formed instead. The  $\gamma$ -phase was identified in our samples using the JCPDS file card data, although it should be noted that the identification of the  $\gamma$ -polymorph on this basis is not definitive (see the discussion in the paper by Hng et al. [11]).

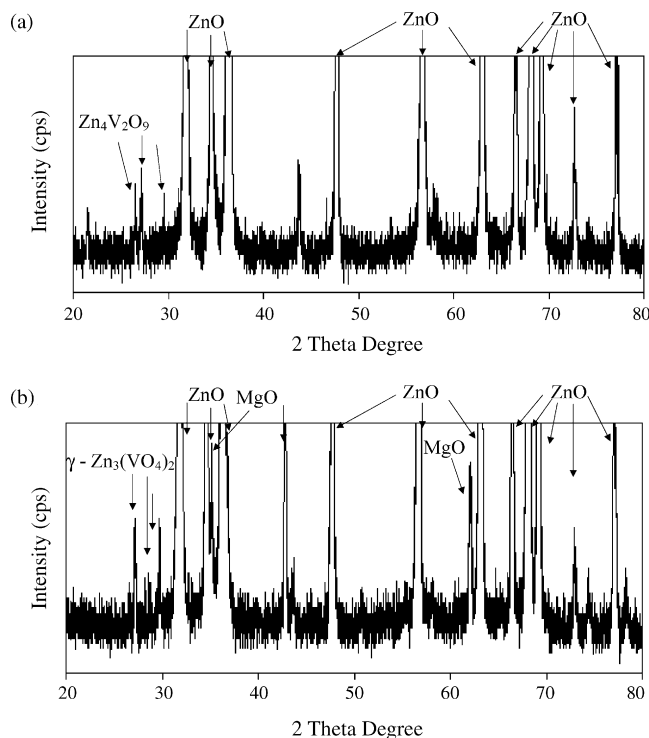


Fig. 1. Typical XRD traces (Cu K $\alpha$ ) for: (a) ZnO–0.5 mol%  $V_2O_5$  (0 mol% MgO) and (b) ZnO–0.5 mol%  $V_2O_5$ –MgO (10 mol% MgO) samples.

For all the samples containing MgO, additional peaks corresponding to the MgO phase was also observed. MgO exhibits limited solubility in the ZnO as evidenced from previous works [13,14], where a maximum of 4 mol% of MgO can dissolve in the ZnO phase at 1573 K at atmospheric pressure.

#### 3.2. Microstructural observations

Low magnification SEM images revealing the typical microstructure of  $V_2O_5$ -doped ZnO varistors are shown in Fig. 2. The binary system (ZV) showed exaggerated ZnO grain growth which previous studies have also reported [5–7]. However, the addition of sufficient amount of MgO yields a small-grained ceramic. The addition of MgO has also reduced the abnormal grain growth that is often observed in ZnO– $V_2O_5$  systems.

The average ZnO grain sizes shown in Table 1 were obtained from the SEM micrographs by multiplying the average linear intercept length of the grains by 1.56 [15]. The initial addition of MgO to ZnO–0.5 mol%  $V_2O_5$  ceramics brought about a significant decrease in grain size. Subsequent increase in MgO content from 10 to 40 mol% showed a gradual decrease in grain size to about 4  $\mu$ m. MgO is a well-known densification aid and grain growth inhibitor for the sintering of  $Al_2O_3$  [16], and it has also been used successfully as a grain size inhibitor in ZnO– $Bi_2O_3$  varistor systems [9].

#### 3.3. Current–voltage characteristics

The effect of MgO addition on the electrical properties of the  $V_2O_5$ -based ZnO materials were characterised by their electric field–current density ( $E$ – $J$ ) properties. Typical  $E$ – $J$  curves are shown in Fig. 3. The corresponding parameters obtained from these curves are summarised in Table 1, where the point at which non-linearity begins is given by the onset electric field  $E_{1\text{ mA/cm}^2}$  and leakage current density  $J_{\text{leak}}$ .

The effects of MgO content on the various electrical parameters are presented graphically in Fig. 4 together with the effect on the average ZnO grain size. The leakage current density  $J_{\text{leak}}$  is not affected much by the addition of MgO. However, the onset electric field  $E_{1\text{ mA/cm}^2}$  and the non-linear coefficient  $\alpha$  are greatly affected by the MgO content. As the amount of MgO is increased, the  $E_{1\text{ mA/cm}^2}$  values increase. This is consistent with the observed decrease in average ZnO grain size as MgO content increases. MgO addition slows down the grain growth, and this increases the number of barriers per unit thickness, and hence increases the  $E_{1\text{ mA/cm}^2}$  values. The non-linear coefficient  $\alpha$ , on the other hand, exhibits a different trend. Initial addition of 2 mol% MgO does not have much effect on the  $\alpha$  value. When MgO is increased to 10 mol% MgO, a significant increase in the  $\alpha$  value is observed. However, subsequent addition of MgO cause a decrease in the  $\alpha$  value. The existence of an optimum MgO content to obtain a high  $\alpha$  value was also reported by Smith et al. [9] in their work on the effects of MgO on

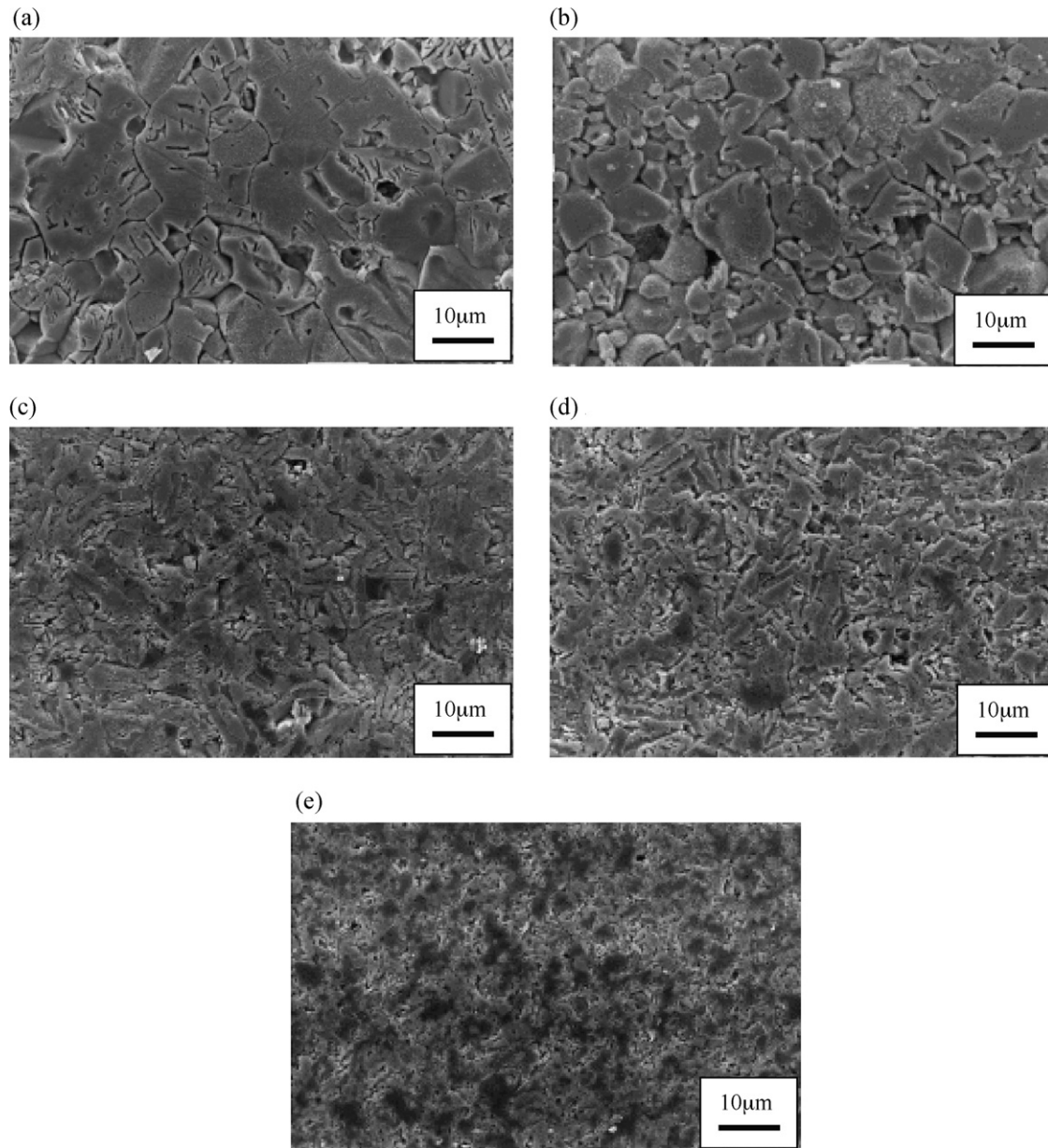


Fig. 2. SEM micrographs of  $V_2O_5$ -doped ZnO varistors containing various amounts of MgO: (a) 0 mol%; (b) 2 mol%; (c) 10 mol%; (d) 20 mol%; (e) 40 mol%.

Table 1

Summary of sample composition, average ZnO grain size and electrical results for the different ZnO– $V_2O_5$ –MgO varistor ceramics

Sample	Composition	Average ZnO grain size ( $\mu\text{m}$ )	$E_{1 \text{ mA/cm}^2}$ (V/cm) <sup>a</sup>	$J_{\text{leak}}$ ( $\times 10^{-4}$ A/cm <sup>2</sup> ) <sup>b</sup>	Non-linear coefficient, $\alpha^c$
ZVM0	ZnO–0.5 mol% $V_2O_5$	17.5	240	6.3	4.3
ZVM2	ZnO–0.5 mol% $V_2O_5$ –2 mol% MgO	9.8	450	6.9	4.1
ZVM10	ZnO–0.5 mol% $V_2O_5$ –10 mol% MgO	6.0	850	7.7	8.7
ZVM20	ZnO–0.5 mol% $V_2O_5$ –20 mol% MgO	5.2	850	7.5	4.3
ZVM40	ZnO–0.5 mol% $V_2O_5$ –40 mol% MgO	4.0	1200	5.9	2.9

<sup>a</sup> Electric field at 1 mA/cm<sup>2</sup>.

<sup>b</sup> Current density at  $0.8E_{1 \text{ mA/cm}^2}$ .

<sup>c</sup>  $\alpha = \log(J_2/J_1)/\log(E_2/E_1)$  where  $J_1 = 1 \text{ mA/cm}^2$  and  $J_2 = 10 \text{ mA/cm}^2$ .

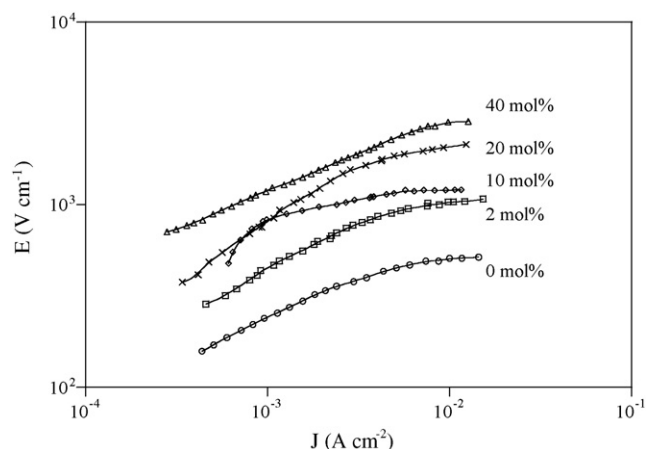


Fig. 3. The electric field–current density ( $E$ – $J$ ) curves for the various ZnO–V<sub>2</sub>O<sub>5</sub>–MgO samples.

ZnO–Bi<sub>2</sub>O<sub>3</sub> system. They observed a decrease in the  $\alpha$  value when 1 mol% of MgO was added, and a maximum  $\alpha$  value of 17 was obtained at 13.2 mol% of MgO, which decreased eventually as MgO content increased.

It should be noted that the maximum  $\alpha$  value obtained in the current study for the V<sub>2</sub>O<sub>5</sub>-doped ZnO varistors is far below that of commercially available Bi<sub>2</sub>O<sub>3</sub>-doped multi-component ZnO varistors. However, from the current study, we have

managed to control the abnormal ZnO grain growth in the V<sub>2</sub>O<sub>5</sub>-doped ZnO system, which allows the use of a much lower sintering temperature of 900 °C as compared to the Bi<sub>2</sub>O<sub>3</sub>-doped ZnO varistor system. Hence, further work can now be done to enhance the varistor performance by composition optimisation with the addition of transition metal oxides to produce multi-component V<sub>2</sub>O<sub>5</sub>-doped ZnO varistor system.

#### 4. Conclusion

MgO was found to be effective as a densifying aid and grain growth inhibitor in ZnO–V<sub>2</sub>O<sub>5</sub>. Addition of MgO to the binary ZnO–0.5 mol% V<sub>2</sub>O<sub>5</sub> system controlled the abnormal ZnO grain growth, and the average ZnO grain size reduced significantly to about 4  $\mu$ m when 40 mol% of MgO was added. The electrical properties deteriorated when more than 10 mol% MgO was added. A maximum non-linear coefficient of 8.7 was obtained for the sample containing 10 mol% MgO in 0.5 mol% V<sub>2</sub>O<sub>5</sub>-doped ZnO varistor. Hence, it can be concluded that in order to achieve optimum electrical properties and at the same time control the ZnO grain growth in V<sub>2</sub>O<sub>5</sub>-doped ZnO varistors, only up to 10 mol% MgO can be added. Based on the current results, further work can now be done to enhance the varistor performance through the addition of transition metal oxides to produce multi-component V<sub>2</sub>O<sub>5</sub>-doped ZnO varistor system.

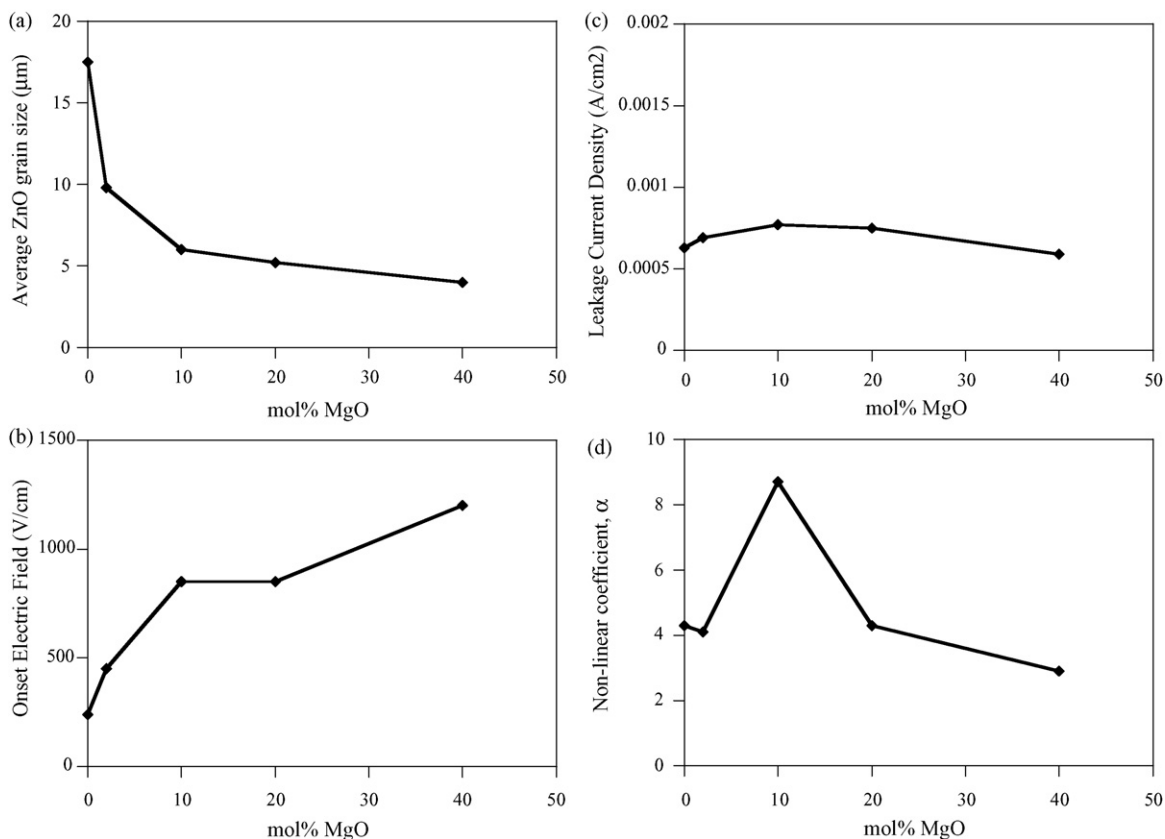


Fig. 4. Effects of MgO content on: (a) average ZnO grain size; (b) onset electric field,  $E_{1\text{mA/cm}^2}$ ; (c) leakage current density,  $J_{\text{leak}}$ ; (d) non-linear coefficient,  $\alpha$ .

## References

- [1] M. Matsuoka, Non-ohmic properties of zinc oxide ceramics, *Jpn. J. Appl. Phys.* 10 (1971) 736–746.
- [2] T.K. Gupta, Applications of zinc oxide varistors, *J. Am. Ceram. Soc.* 73 (1990) 1817–1840.
- [3] E. Olsson, G.L. Dunlop, The effect of  $\text{Bi}_2\text{O}_3$  content on the microstructure and electrical properties of ZnO varistor materials, *J. Appl. Phys.* 66 (1989) 4317–4324.
- [4] A.B. Alles, V.L. Burdick, The effect of liquid-phase sintering on the properties of  $\text{Pr}_6\text{O}_{11}$ -based varistors, *J. Appl. Phys.* 70 (1991) 6883–6890.
- [5] J.K. Tsai, T.B. Wu, Microstructure and nonohmic properties of binary ZnO– $\text{V}_2\text{O}_5$  ceramics sintered at 900 °C, *Mater. Lett.* 26 (1996) 199–203.
- [6] H.H. Hng, K.M. Knowles, Characterisation of  $\text{Zn}_3(\text{VO}_4)_2$  phases in  $\text{V}_2\text{O}_5$ -doped ZnO varistors, *J. Eur. Ceram. Soc.* 19 (1999) 721–726.
- [7] H.H. Hng, K.M. Knowles, Microstructure and current–voltage characteristics of multicomponent vanadium-doped zinc oxide varistors, *J. Am. Ceram. Soc.* 83 (2000) 2455–2462.
- [8] J. Wu, C.S. Xie, K.J. Huang, A.H. Wang, W.Y. Wang, Low temperature sintering of doped ZnO– $\text{V}_2\text{O}_5$  varistors, *J. Inorg. Mater.* 19 (2004) 239–243.
- [9] A. Smith, G. Gasgnier, P. Abélard, Voltage–current characteristics of a simple zinc oxide varistor containing magnesia, *J. Am. Ceram. Soc.* 73 (1990) 1098–1099.
- [10] J.J. Brown, F.A. Hummel, Reactions between ZnO and selected oxides of elements of groups IV and V, *Trans. Br. Ceram. Soc.* 64 (1965) 419–437.
- [11] H.H. Hng, K.M. Knowles, P.A. Midgley, Zinc vanadates in vanadium oxide-doped zinc oxide varistors, *J. Am. Ceram. Soc.* 84 (2001) 435–441.
- [12] M. Kurzawa, I. Rychlowska-Himmel, M. Bosacka, A. Blonska-Tabero, Reinvestigation of phase equilibria in the  $\text{V}_2\text{O}_5$ –ZnO system, *J. Therm. Anal. Cal.* 64 (2001) 1113–1119.
- [13] M. Kunisu, I. Tanaka, T. Yamamoto, T. Suga, T. Mizoguchi, The formation of a rock-salt type ZnO thin film by low-level alloying with MgO, *J. Phys.: Condens. Matter* 16 (2004) 3801–3806.
- [14] N.B. Chen, C.H. Sui, Recent progress in research on  $\text{Mg}_x\text{Zn}_{1-x}\text{O}$  alloys, *Mater. Sci. Eng. B* 126 (2006) 16–21.
- [15] M.I. Mendelson, Average grain size in polycrystalline ceramics, *J. Am. Ceram. Soc.* 52 (1969) 443–446.
- [16] R.L. Coble, U.S. Pat. No. 3,026,210, March 20 (1962).